



Swansea University
Prifysgol Abertawe



Cronfa - Swansea University Open Access Repository

This is an author produced version of a paper published in:

Journal of Plankton Research

Cronfa URL for this paper:

<http://cronfa.swan.ac.uk/Record/cronfa40800>

Paper:

Munk, P., Nielsen, T., Jaspers, C., Ayala, D., Tang, K., Lombard, F. & Riemann, L. (2018). Vertical structure of plankton communities in areas of European eel larvae distribution in the Sargasso Sea. *Journal of Plankton Research* <http://dx.doi.org/10.1093/plankt/fby025>

This item is brought to you by Swansea University. Any person downloading material is agreeing to abide by the terms of the repository licence. Copies of full text items may be used or reproduced in any format or medium, without prior permission for personal research or study, educational or non-commercial purposes only. The copyright for any work remains with the original author unless otherwise specified. The full-text must not be sold in any format or medium without the formal permission of the copyright holder.

Permission for multiple reproductions should be obtained from the original author.

Authors are personally responsible for adhering to copyright and publisher restrictions when uploading content to the repository.

<http://www.swansea.ac.uk/library/researchsupport/ris-support/>

1 Vertical structure of plankton communities in areas of
2 European eel larvae distribution in the Sargasso Sea.

3

4 Peter Munk^{1*}, Torkel Gissel. Nielsen¹, Cornelia Jaspers^{1,2}, Daniel J. Ayala¹, Kam W. Tang³, Fabien
5 Lombard⁴, Lasse Riemann⁵.

6 1. National Institute of Aquatic Resources, Technical University of Denmark, 2800 Lyngby,
7 Denmark

8 2. Helmholtz Centre for Ocean Science, GEOMAR, 24105 Kiel, Germany

9 3. Department of Biosciences, Swansea University, Swansea, SA2 8PP, United Kingdom

10 4. Sorbonne Université, CNRS-INSU, Laboratoire d'Océanographie de Villefranche, LOV UMR
11 7093, F-06230 Villefranche-sur-mer, France

12 5 Marine Biology Section, Department of Biology, University of Copenhagen, 3000 Helsingør,
13 Denmark

14

15 Keywords: vertical migration, plankton communities, leptocephali larvae, freshwater eels,
16 Subtropical Convergence Zone

17

18 Running title: Vertical structure of plankton in the Sargasso Sea

19

20 *Corresponding author: Peter Munk. E-mail address: pm@aqua.dtu.dk

21

22 **Abstract**

23 The European and American eels spawn in the Subtropical Convergence Zone (STCZ) in the
24 Sargasso Sea, a dynamic and relatively productive area that is strongly influenced by front and eddy
25 formations and subducted high-saline water masses. To understand how the physical and biological
26 environments may affect the early life history of eels, we conducted a detailed bio-physical
27 investigation of the water column at a site of high eel larvae abundance. Diel measurements and
28 sampling in the upper 300 m revealed strong variations in hydrographic conditions and mean depths
29 of different taxonomic groups; however, characteristic patterns of distribution were apparent. Most
30 species showed diel vertical migrations, ascending about 20-30 m at night, whereas examples of
31 nighttime downward migration were also seen. European eel larvae were among the species
32 showing more extensive diel vertical migration: their population mean depth changed from 160 m at
33 day to 100 m at night where abundance peaked at 45 m depth. Distribution and migration of eel
34 larvae corresponded to patterns observed for small hydrozoans, supporting a proposed predator-prey
35 linkage. The study demonstrates the diverse and vertically strongly structured plankton community
36 of STCZ where larvae of eel and other fish find a wide range of potential niches.

37

38

39 **Introduction**

40 The Subtropical Convergence Zone (STCZ) in the Sargasso Sea is known to be a hotspot for
41 spawning of Atlantic eels (Schmidt, 1923; Miller, 2014). Due to a sharp decline in recruitment to
42 the eel populations in the recent decades, there is a strong demand for further understanding of the
43 temporal and spatial variabilities in the bio-physical characteristics of the zone and how they may
44 influence recruitment success. In the STCZ, warm tropical water meets colder North Atlantic water
45 masses and the zone is bordered by hydrographic fronts of changing intensity and location (Eriksen
46 *et al.*, 1991, Ullman *et al.*, 2007). Furthermore, the STCZ is characterized by significant eddy
47 formation (Halliwell *et al.*, 1991) leading to intensive mixing in the upper 200-300 m (Munk *et al.*,
48 2010; Richardson and Bendtsen, 2017). While the deep current (the North Equatorial Current) is
49 directed towards the west, the upper layers in the zone might in some areas flow north-east along
50 the zonal density fronts, forming an eastward Subtropical Counter Current (SCC) (Cushman-Roisin,
51 1984). A thermocline is present at 100-150 m and an intrusion of more saline water originating
52 from the equatorial areas is often seen at 80-150 m (Williams, 2001). The pronounced variability in
53 the horizontal and vertical hydrography is likely to affect the structuring of plankton communities in
54 the area with further influence on the early development of the anguillid eels (*Anguilla anguilla* and
55 *A. rostrata*).

56 Studies of the plankton communities in the Sargasso Sea often target areas north of the STCZ, in
57 particular the site of the Bermuda Atlantic Time-series Study (BATS) (reviewed by Steinberg *et al.*,
58 2001). Conditions in these colder north-Atlantic waters are, however, not comparable to the STCZ,
59 where the different hydrography would favor different plankton communities (Longhurst, 1985).
60 Studies specifically targeting central areas of the STCZ have found an enhanced abundance of
61 primary producers (Riemann *et al.*, 2011) and elevated productivity (Richardson and Bendtsen,
62 2017). Although the Sargasso Sea is generally considered as oligotrophic with a predominance of
63 picoplankton (Gasol *et al.*, 1997), the biomass of large protists, such as athecate dinoflagellates and
64 ciliates, has been found to equal or exceed that of picoplankton within the STCZ (Riemann *et al.*,
65 2011), probably leading to a locally enhanced mesozooplankton production. An enhancement in a
66 number of metazoan groups, e.g. copepods and appendicularians, has been observed in central areas
67 on STCZ (Munk *et al.*, 2010; Andersen *et al.*, 2011). Furthermore, fish larvae including those of
68 European and American eels have been found in relatively high abundances within STCZ, with

69 declining abundances when passing the fronts towards waters outside the STCZ (Ayala *et al.*,
70 2016).

71 In addition to horizontal variability in plankton community composition and abundances in the
72 STCZ, variability is also apparent along the vertical axis, where most plankton taxa are
73 concentrated in specific depth strata (Riemann *et al.*, 2011; Andersen *et al.* 2011). The published
74 information on vertical distribution of fish larvae in the STCZ is restricted to distributional patterns
75 of leptocephali larvae. In the western Sargasso, Miller (2015) found the majority of leptocephali
76 larvae in the upper 100 m at night, with several species (including *Anguilla rostrata*) concentrated
77 within the 50-60 m depth. Likewise, Castonguay and McCleave (1987) observed that at nighttime,
78 *Anguilla* spp. larvae were concentrated within 50-70 m. *Anguilla* spp. larvae have been observed to
79 perform marked diel vertical migrations, descending to 100-200 m depth during the day (Schoth
80 and Tesch, 1982). However, only a few eel larvae have been found below a depth of 200 m
81 (Schmidt, 1923; Castonguay and McCleave, 1987).

82 The early life of fishes in the STCZ, including the *Anguilla* spp., is governed by the specific
83 physical, chemical and biological characteristics of available habitats in the water column. In order
84 to gain further understanding of opportunities and constraints to the life of *Anguilla* spp. larvae, we
85 here investigate in detail the water column properties and the structuring of the plankton community
86 of the STCZ, looking for commonalities and differences between community members. We
87 included several trophic levels, ranging from algae and microplankton, to mesozooplankton and
88 macroplankton, and finally onto the fish larvae. The study was carried out during a larger field
89 investigation at a site of relative high abundances of *Anguilla* spp, and we hypothesized that the eel
90 larvae occupy a specific niche in the community, defined by their vertical position, their diel
91 migration pattern and their linkages to specific hydrographical and biological characteristics.

92

93 **Materials and methods**

94 Intensive sampling was conducted at 25°38' N, 62°48'W from 31 March 13:46 UTM to 1 April
95 14:20 UTM, 2014 on board of the R/V Dana (local time was UTM – 4 hours). The site was part of a
96 survey transect across the STCZ, extending along 62°45'W from 24°40'N to 29°50'N (Fig. 1), and
97 was chosen for the relatively high *A. anguilla* abundances observed during the standard transect
98 sampling.

99 Profiles of temperature, salinity, fluorescence, oxygen and irradiance were measured from surface
100 to 400 m depth by a Seabird SBE11 (9+) CTD, with mounted Biospherical QSP-2300L PAR
101 Sensor, SBE 43 Dissolved Oxygen Sensor, and Turner Cyclops-7 Fluorometer. Silicate, nitrite,
102 nitrate and chlorophyll *a* were measured in subsamples from ten-liter Niskin bottle samples taken at
103 10, 30, 60, 85, 130, 155, 255 and 400 m depths.

104 An Underwater Video Profiler (UVP5, serial number Sn003, pixel size ca. 0.147; Picheral *et al.*,
105 2010) was deployed alongside the CTD to 400 m. The device emitted flashes of red LED light that
106 illuminated 0.93L of the water. Images of all particles within the illuminated area were recorded
107 and analyzed for abundances in defined size ranges. Objects larger than 30 pixels were further
108 analyzed by a taxonomist. Here we only report observations of particles in three size ranges: small
109 (0.05-0.53 mm), medium (0.53-1.06 mm), and large (1.06-4.0 mm).

110 Microzooplankton (ciliates and heterotrophic dinoflagellates) were analyzed using water
111 subsamples from ten-liter Niskin bottle samples taken at 10, 30, 60, 85, 130, 155, 255 and 400 m
112 depths. These were immediately fixed with acid Lugol's solution (2% final concentration) and
113 stored in the dark at 5°C until analysis. For the analysis, protozoans were allowed to settle for 24 h
114 in 50-ml sedimentation chambers, and were then enumerated and sized under an inverted
115 microscope (Utermöhl, 1958). Cells were identified to the lowest possible taxonomic level and
116 grouped by equivalent spherical diameter intervals of 10 µm. Cell volumes were estimated from
117 appropriate geometric formulae and converted to carbon content. All athecate dinoflagellates of
118 unknown trophic type were considered heterotrophic (Andersen *et al.*, 2011).

119 Zooplankton samples were collected using a multiple opening-and-closing net (Multinet Midi,
120 HydroBios[®], 0.25 m² mouth opening) in seven discrete depth intervals (0-25, 25-65, 65-100, 100-
121 135, 135-180, 180-230 and 230-280m). Zooplankton in the micro- and mesozooplankton size range
122 were sampled by hauling vertically a 45 µm mesh Multinet from 280 m to the surface, while rare
123 and larger sized zooplankton were sampled during an oblique haul with a 335 µm mesh Multinet
124 lowered to 280 m and retrieved to the surface at a speed of 2 knots. For the 45 µm Multinet
125 sampling, the water volume filtered per net ranged from 5 to 13 m³. Samples were preserved in 4%
126 Borax buffered formalin, and after the cruise the zooplankton were identified, enumerated and
127 measured for total length, and cephalothorax length for copepods.

128 Fish larvae and gelatinous macrozooplankton were sampled using a conical ring net (MIK, 3.5 m
129 diameter opening, 25 m total length, 560 μm body mesh size with 330 μm mesh for the hindmost 1
130 m and the cod end). The net was lowered to a given depth, measured by a mounted depth sensor
131 (Scanmar[®]), using a fast wire pay-out, and towed at 2 knots for 40 min. Tow depth varied by ± 3 m
132 during tows. Afterward, the net was retrieved at a high speed. Filtrating during the pay-out and
133 retrieval phase was assumed to be ineffective at such high speed. The effective volume filtered was
134 estimated from the tow path at depth apparent from the recorded profile of the depth sensor. Six
135 discrete depths were sampled (45, 85, 120, 155, 205 and 255 m) during day (12:00-18:00 local
136 time) and night (00:00-06:00 local time). Upon retrieval, the net was washed down and the cod-end
137 content was transferred to 20 L transparent buckets (Cambro[®]). The buckets were kept on ice
138 during processing, and the content was examined for fish larvae and gelatinous macrozooplankton
139 (excluding siphonophores) within 45 min.

140 Gelatinous zooplankton were identified and measured alive using a dark field light table in
141 transparent plexi-glass trays. After the screening, 10% of the MIK sample was preserved in 4%
142 buffered formalin solution for later estimation of siphonophore abundance. Siphonophore
143 abundance was difficult to estimate due to their colonial structure and tendency to disintegrate.
144 However, the sampled siphonophore community consisted primarily of Calycothorans, hence we
145 used only the anterior nectophore of the polygastric stage for species identification and enumeration
146 (Bouillon *et al.*, 2004). Very few bracts of the sexual eudoxid stage were encountered.

147 Observed fish larvae were directly preserved in 96% ethanol, the leptocephali after being length
148 measured in a stereomicroscope-video setup. The remainder of the sample was preserved in ethanol
149 for later sorting, identification and measurement of fish larvae that were not observed during the
150 initial screening. All length measurements were made to larval standard length. Fish larvae visually
151 identified as *Anguilla* spp. were later verified as either *A. anguilla* or *A. rostrata* using molecular
152 markers (Jacobsen *et al.*, 2016). Identification of other larval fish species was based on type
153 specimens from an earlier study in the same area (Ayala *et al.*, 2016).

154 Information on the distribution and diel migration of acoustically reflecting organisms were
155 obtained from a ship-mounted Simrad[®] EK60 38 kHz echosounder, which was run continuously
156 during the vertical study. Signals were analyzed by Echoview[®] software, and data on volume
157 backscatter at depth were interpolated using the Surfer[®] program.

158 *Data analyses:*

159 Distributional mean depths (MD) of plankton size intervals, genera or species were calculated as:

$$160 \quad MD = \sum_{k=0}^n D_k * W_k * C_k / \sum_{k=0}^n W_k * C_k$$

161 Where D_k is mean depth of stratum k (m), W_k is width of stratum k (m) and C_k is the estimated
162 density of organisms in stratum k (no m^{-3}).

163 For analysis of commonalities and differences in vertical distributions of plankton taxa we
164 calculated a similarity matrix combining a double hierarchical classification and an ordered
165 heatmap representation. The method considered Euclidean distances with a “complete link”
166 classification. To compare both abundant and non-abundant taxa we used proportions in strata and
167 solely strata in 45 m and below, since some taxa were not sampled in the uppermost stratum. In a
168 schematic representation, the taxa were organized and grouped according to similarity in their
169 relative abundances at depth.

170

171 **RESULTS**

172 *Hydrography*

173 The sampling site was positioned ca. 100 km north of the southern front of the STCZ. This front
174 was characterized by declining isotherms at the southernmost part of the transect (Fig. 1 b). Water
175 temperature was ca. 24-24.5°C in a mixed water layer extending to about 80 m depth. Below this
176 layer a wide thermocline was apparent, with a decline in temperature to 19°C at 150 m (Fig. 2 a).
177 Salinity was 36.6 in the mixing zone, and deeper, between 80 and 160 m depth, an intrusion of more
178 saline water (~ 36.8) was apparent (Fig 1 c, Fig. 2 a). The intrusion at this sampling site had a
179 double structure, a pattern also observed at other stations during the cruise. Further below the
180 salinity declined, reaching 36.42 at 400 m and continuing the decline until at least the depth of 1000
181 m (nearby CTD cast, data not shown).

182 Light levels measured at 14:30 UTM declined from 1000 $\mu\text{mol m}^{-2}\text{s}^{-1}$ at 10 m to 40 $\mu\text{mol m}^{-2}\text{s}^{-1}$ at
183 100 m and 1.5 $\mu\text{mol m}^{-2}\text{s}^{-1}$ at 160 m (Fig. 2 b), and were below the detection limit at depths below
184 250 m. The attenuation coefficient varied through the water column, showing peaks in the
185 immediate surface layer and the in association with the deep chlorophyll *a* layer (Fig. 2 b).

186 Dissolved oxygen level was near 100% saturation in the upper 100 m but showed an abrupt drop to
187 about 80 % across the upper thermocline, and stayed at this level further below (Fig. 2 b).
188 Nitrate+nitrite levels were low in the upper 110 m ($< 0.25 \mu\text{mol L}^{-1}$), increased to $2 \mu\text{mol L}^{-1}$ at 130
189 m and increased further at greater depths (Fig. 2 c). Silicate levels were in the order of $1\text{-}2 \mu\text{mol L}^{-1}$,
190 but were markedly lower between 60 and 130 m (Fig. 2 c).

191 *Microplankton and snow particles*

192 The CTD fluorometer and extracted chlorophyll measurements showed similar vertical profiles of
193 algal concentrations (Fig. 2 d). In the mixing zone at 0-80 m depth, the chlorophyll *a* concentration
194 was low ($\sim 0.08 \mu\text{g L}^{-1}$), but it increased further below and peaked in a deep chlorophyll maximum
195 (DCM) of $0.32 \mu\text{g L}^{-1}$ at about 120 m depth. Below the DCM the chlorophyll *a* concentration
196 declined markedly to near zero at 200 m depth.

197 Particles detected by the Underwater Vision Profiler (UVP) were categorized into three groups
198 based on their equivalent spherical diameter (Fig. 3 a). All three groups were found in high
199 abundances near the surface, but they differed in their vertical distributions throughout the water
200 column. Small particles showed a subsurface minimum of ~ 15 particles L^{-1} in the depth range 20-60
201 m, increasing to 25 particles L^{-1} at 160-200 m. In contrast, abundances of both medium and large
202 particles steadily decreased with depth, reaching near zero particles below 250 m. Two
203 characteristic components of the medium and large sized particles were identified as
204 *Trichodesmium* colonies and radiolarians (Rhizaria) (Fig. 3 b). Both of these showed highest
205 abundances above 60 m with another enhancement in abundance at 120-140 m (Rhizaria) or 140-
206 200 m (*Trichodesmium*). Concentrations of ciliates and heterotrophic dinoflagellates based on bottle
207 sampling showed both their highest levels above 150 m, but their peaks of abundance in the water
208 column differed (Fig. 3 c). The dinoflagellates peaked close to the DCM, while abundances of
209 ciliates were high in the mixed layer and showed a secondary peak below the DCM.

210 *Mesozooplankton*

211 The vertical profile of total mesozooplankton from the $45 \mu\text{m}$ Multinet sampling showed a
212 characteristic peak at the surface, another at the 65-100 m depth interval, and very low abundances
213 below 180 m (Fig. 4 a, Suppl. table 1). Diel changes in the combined vertical distribution of the
214 community in the investigated upper 250 m were marginal, with a weak tendency of nighttime
215 descent. There was, however, great variability in distribution patterns among the different

216 taxonomic groups (Suppl. fig. 1, Suppl. table 1). For example, *Oncaea* sp. showed no surface peak,
217 (Fig. 4 g-h), while *Oithona* sp. copepods (Fig. 4 c) were distributed relatively deep with a peak
218 around 150 m. Hydrozoans as *Amphicaryon acaule* and *Bougainvillia niobe* were distributed deep
219 at day and shallower at night (Fig. 4 k-l). Additional differences were apparent within taxa for the
220 naupliar and copepodite stages of copepods; e.g. *Clausocalanus* spp. nauplii tended to be deeper
221 (Fig. 4 e-f) while *Oithona* sp. nauplii tended to be shallower (Fig. 4 c-d) compared to the respective
222 copepodite stages.

223 The vertical distributions and migration patterns of mesozooplankton were related to size of
224 organisms (Fig. 5 a). There was a general decline in MD, both for the copepods and for the group of
225 other mesozooplankton. For the copepods the MD was about 70 m for length <500 μm , and at these
226 sizes (including the nauplii stages) the distances of diel vertical migration (DVM) were minor
227 (<10m). In the copepod length range of 500-1000 μm the MD declined from the 70 to 90 m depth,
228 with a DVM of 20-30 m (ascent at night). The largest size group for which the MD could be
229 calculated (1300 μm) was found at depth 110-140 m and showed a nighttime descent; this group was
230 dominated by *Haploptilus* spp, which had an uncommon DVM behavior (Fig 5 b-c). In the group of
231 non-copepod zooplankton, there was a more pronounced influence from size, and MD changed
232 from 20-60 m to 90-130 m across the length range 100-900 μm , while the DVM was 10-50 m,
233 primarily with an ascent at night.

234 Underlying the apparent size-dependence of MD and DVM for copepods, there was a significant
235 variability in MD and DVM related to stage and taxon. There was a span in MD from 40-50 m for
236 copepodite stages of *Acartia* sp. and *Clausocalanus* sp., to 180-200 m for *Marmonilla* sp. and
237 *Pleuromamma* sp. (Fig. 5 b). Between these extremes, the MD's of the other taxa were spread quite
238 evenly. The general range of DVM was 10-20 m, but examples of a wider range of migration were
239 also seen (Fig. 5 b-c). Our findings also showed that adults of different species of the same genera
240 can behave quite differently, e.g. *Clausocalanus paulus* vs. *C. furcatus*. and *Oncaea media* vs. *O.*
241 *mediterranea* (Fig. 5 c). This appears, however, not to be in accordance with the general tendency
242 of larger size being at greater depth, given that *Clausocalanus paulus* is smaller than *C. furcatus*
243 (~560 μm vs. ~800 μm) and *Oncaea media* is smaller than. *O. mediterranea* (~370 μm vs. ~660
244 μm).

245 *Macroplankton*

246 Most of the macroplankton caught by the large ring net were distributed relatively deep at day
247 between 80 and 180 m, and shallower at night above 120 m (Suppl. table 1). For some taxa within
248 this group, the abundances integrated for the sampled water column were higher during night than
249 during day. Net avoidance at day is unlikely the explanation because these macroplankton cannot
250 visually detect the approaching net; rather, a part of the population may be distributed deeper than
251 our sampling depth at daytime. *Bougainvillea niobe* was among the most numerically abundant; this
252 species migrated from about 130 m at day to 90 m at night (Fig. 4 m). The siphonophore
253 *Amphicaryon acaule* showed a strong upward shift in MD from about 160 m to 70 m between day
254 and night (Fig. 4 n). Other siphonophores stayed deeper during nighttime, and their MD changed
255 from about 150 m at day to 110 m at night (Fig. 4 o).

256 *Leptocephali larvae*

257 We collected 164 *A. anguilla* and 19 *A. rostrata* larvae during the two series of ring net hauls. The
258 vertical distribution of *A. anguilla* showed a pronounced diel difference: larval abundance peaked at
259 155 m in daytime (82% of larvae were sampled in the two depth strata 120 m and 155 m), but at
260 nighttime larval abundance peaked at 45 m (53% of larvae present at the stratum 45 m; Fig 6 a), and
261 was also more dispersed in the water column. The MD at day was close to the observed depth of
262 peak concentration (160 m vs 155 m), while at night the MD was somewhat deeper (110 m vs 45 m)
263 (Fig. 8 a). Although the diel patterns of vertical distribution of *A. rostrata* were less apparent due to
264 the relatively low catch of this species, findings also indicate peaks in densities at 155 m at day and
265 at 45 m at night (Fig. 6 b), while the MD's are slightly shallower than for *A. anguilla* (150 m at day
266 and 90 m at day, Fig 8 a). Mean body lengths for *A. anguilla* were 14.1 and 14.5 mm in daytime
267 and nighttime samples, respectively, and for *A. rostrata* 14.4 and 17.5 mm, respectively. Larval
268 mean lengths tended to increase with depth at day, whereas no such tendency was seen at night
269 (Fig. 6 d-f).

270 Other species of leptocephali larvae were generally larger than the anguillid leptocephali, and due to
271 visual net avoidance they were poorly represented in the daytime samples. Only the nighttime
272 vertical distribution of the combined group of leptocephali larvae is presented here, illustrating the
273 same pattern as for the anguillid larvae: increasing density towards the shallowest stratum of
274 sampling (Fig. 6 c).

275 *Other fish larvae*

276 We identified 16 taxonomic groups of fish larvae other than the leptocephali; these were identified
277 to the species or family level (Suppl. table 1). The diel vertical distribution differed markedly
278 between several of these groups (Fig. 7): Some had their peak distribution at day in the mid-layer
279 (depths 120-155 m) but the concentration could locally be high with almost all larvae found at the
280 same depth (e.g. *Hygphum taaningi*, Fig. 7 e), or the larvae could be more dispersed in the lower
281 water column (e.g. *Scopelarchus* sp., Fig. 7 b). At night, the overall majority of individuals of each
282 taxon was found at the shallowest depth (e.g. *Evermannellidae* spp., Fig. 7 a), in the mid-layer (e.g.
283 *Sternoptychidae diaphana*, Fig. 7 f) or at the deepest depth investigated (*Scopelarchus* sp., Fig. 7 b).
284 The large variation in distribution patterns of larvae was reflected in their MD's (Fig. 8 b): two
285 species were either outstandingly shallow (*Ceratoscopelus warmingii*) or deep (*Scopelarchus* sp.),
286 whereas the mean depths of the others were distributed quite evenly between 70 m and 170 m. Both
287 downward and upward migrations between day and night were observed, the vertical migration
288 range was for most species in the order of 20-30 m, but a few species migrated 40-50 m (Fig. 8 b).

289

290 *Fish and other organisms from acoustics*

291 The vertical distribution of organisms reflecting 38 kHz signals was described for a 48-h period,
292 from 1:00 on the 31 March to 23:00 on the 1st April (Fig. 9). At night, acoustic reflections showed
293 an elevated abundance of organisms in the upper 140 m. Separate layers of enhanced reflection
294 were apparent. Just before daybreak (> 10 PAR at 10:00 UTM), a group of organisms descended
295 relatively quickly, reaching ~300 m at 10:30 and ~500 m at 12:00. In contrast, other organisms from
296 the series of bands within the upper 250 m showed a more gradual and shorter descent (max. ~50 m
297 descent of separate band), reaching their deepest level at noon when light intensity was at its
298 highest. These migration patterns were reversed after 12:00 UTM, and were repeated in the
299 following 24 h period (Fig. 9).

300 *Plankton community patterns*

301 A cluster analysis on vertical distribution of all abundant mesozooplankton and ichthyoplankton
302 taxa illustrated the diversity of distribution patterns, but also revealed a separation of taxa into
303 distribution types (Suppl. fig. 1). At a “semi R-square” level above 50% we separated 6 clusters of
304 distinct characteristics in the daytime sampling (Suppl. fig. 1 a). Three of these showed a
305 characteristic concentration within a single stratum, one of these types, with a concentration in the

306 85 m stratum, was dominated by mesozooplankton taxa, while fish larvae dominated in two other
307 types (concentration at 45m or 120 m). A large group of taxa was characterized by their bimodal
308 vertical distribution showing peak abundances in the 85 m and 155 m strata; this was the general
309 vertical distribution pattern for most of the mesozooplankton. Another group, in which we find the
310 two anguillid eels, constituted a fifth type showing enhanced abundance in the 120 m and 155 m
311 strata. The sixth group was found relatively deep (in 155 m stratum or below); however, only few
312 taxa exhibited this distribution pattern. The analysis inferred further clusters within these main
313 clusters, and the general picture of the analysis was a high diversity in patterns of plankton
314 distribution.

315

316 **Discussion**

317 Our study was focused on plankton distribution in the upper 250 m of the 5000 m deep water
318 column with the expectation that the majority of the community, including the eel larvae, would be
319 distributed here. This interval covers the euphotic zone of sufficient light for primary production
320 and for visual feeding by the fish larvae (about $0.02 \mu\text{mol m}^{-2} \text{s}^{-1}$; Blaxter, 1980). Further, our
321 observations of a marked decline in abundances of most of the investigated taxa in the deepest
322 sampled stratum (midpoint 255 m) suggests that, by sampling to this depth, we included most of the
323 relevant plankton biomass. The indication in our data that most planktonic organisms in the area
324 had this relatively shallow distribution is supported by findings during studies in other oligotrophic
325 areas which sampled to larger depths (>1000 m). In those studies, modal depths of most
326 investigated plankton species were also found in the interval of 25-150 m (e.g. Longhurst, 1985;
327 Sameoto, 1986). A smaller proportion of the plankton, however, primarily inhabit the deeper
328 layers; e.g. Deevey and Brooks (1977) found in a study off Bermuda that abundances of plankton
329 species residing below 500 m (in the 500-1000 m layer) could be up to 20% of the abundances
330 above 500 m.

331 The high diversity in plankton distributions in the investigated water layer reflected the large
332 variability in physical conditions. Within the first 250 m of the water column there was a significant
333 change in light, temperature and water density, and within the pycnocline (80-150 m) we found a
334 strong peak in chlorophyll *a* and a marked intrusion of relatively high-saline water. Thus a wide
335 range of habitual niches are available to the mesozooplankton and ichthyoplankton, and

336 characteristic peaks of distribution within certain depth strata were seen for many organisms.
337 Consequently, the clustering of organisms based on distributional similarities showed that in
338 addition to bulk-water characteristics, there were also significant fine-scale variabilities that
339 influenced the distributional patterns for both mesozooplankton and ichthyoplankton.

340 A large number of the investigated taxa showed systematic polymodality in their vertical
341 distribution. The layer immediately below the uppermost surface (measured at 45 m depth)
342 appeared unsuitable for most taxa, leading to low abundances here. While the mesozooplankton
343 organisms often were abundant above (12 m stratum) and below (85 m stratum); this led to two
344 modes in the vertical distribution. For many organisms there was a tendency of another low in
345 abundance at the central pycnocline at about 120 m, within the salinity intrusion and the chlorophyll
346 *a* maximum. This tendency of several modes in distribution was seen for much of the
347 mesozooplankton, both during daytime and nighttime sampling, for much of the mesozooplankton,
348 while for the ichthyoplankton the pattern of distribution was unimodal for most taxa.

349 The concentration at specific depth was evident for the two anguillid eel larvae. At daytime, the
350 larvae congregated in the 155 m stratum at a concentration about seven times as high as the average
351 of the other abundance estimates in the water column, and at nighttime the concentration in the 45
352 m stratum was three times as high as the average of other estimates. Thus, at the investigated site,
353 most of the anguillid leptocephali were below 100 m at daytime while the majority migrated to
354 above 100 m depth at night. Interestingly, peaks in eel larvae distribution coincided with peaks in
355 abundances of sampled hydrozoans, as apparent when comparing Fig 6 a-b with Fig. 5 k-l. The
356 hydrozoans have been proposed as possible food items for the leptocephali larvae (Riemann et al.
357 2010), and a study from the same cruise found eel larval gut contents dominated by gene sequences
358 of taxa belonging to Hydrozoa (Ayala et al., in press).

359 The observations of a deeper distribution of anguillid eel larvae during daytime, and a shallower
360 distribution during nighttime are in accordance with other findings for the species during the
361 winter/spring period. Castonguay and McCleave (1987) found significant abundance peaks in
362 specific depth strata as well: In their study, the maximal concentration at depth was seen at night
363 and was here about nine times the average of the other depth strata. Accordingly, the day and night
364 peak concentrations of larvae occurred within the wide pycnocline, and the tendency of an increase
365 in larval mean length with increasing sampling depth during daytime are also apparent in the data
366 presented by Schoth and Tesch (1984).

367 The observed diel migration (~70m) of *Anguilla* sp. was of exceptional magnitude compared to
368 migrations of most other fish larvae in our study, which ranged only 10-30 m. Migration distances
369 of oceanic fish larvae are commonly in the lower range; for example, in a study of the fish larval
370 community off the Canary Islands, Rodriguez *et al.* (2006) observed relatively short migration
371 distances of 5-20 m for most species, and similar to our study, they observed both upward and
372 downward migrations during night. The different species of fish larvae we observed apparently
373 utilized different parts of the water column; some were concentrated in relatively deep water, some
374 in the shallow layer, and others were more dispersed in the mid-layer. Thus, while the vertical
375 distributions of fish larvae overlapped to different degrees, the calculated midpoints of distributions
376 extended throughout much of the water column.

377 We used acoustic measurements and the diel movement of bands of enhanced backscatter to
378 describe migratory patterns of plankton and fish at a finer temporal scale than our day-night
379 sampling. Stratification of the backscatter is a common observation in acoustic surveys, and the
380 different bands of enhanced backscatter have been related to different taxonomic composition of
381 organisms (e.g. Lawson *et al.*, 2004). While we cannot directly link certain bands to specific taxa,
382 the patterns of backscatter in the uppermost water column during night are in accordance with the
383 observations of peaking distributions of organisms in the pycnocline and around the high-saline
384 intrusion at 80-130 m depth (Fig 9).

385 The acoustic observations complement our day-night sampling by showing the diel migration as a
386 gradual descent to, and ascent from, the deepest positions of given organisms. The descent was
387 initiated at the first light at the surface, and the return was finished at time of complete darkness.
388 Successively, the vertical positions of organisms were stable during night, with a slight tendency of
389 deeper distribution at midnight, until a new descent in the morning. From the acoustic
390 measurements the general migration distances in the upper part of the water column were
391 interpreted to be about 50 m, which is in the upper range compared to migration distances of most
392 of the (smaller) organisms that were included in our day-night sampling campaign. The descent of
393 the upper set of distribution bands reached to about 270 m, which is within the range of the general
394 light threshold for larval fish feeding (Fig. 9). In the echogram some bands of acoustic backscatter
395 apparent at night descended much deeper than the 50 m; these are likely related to movement of
396 mesopelagic fish which are commonly observed to descend to more than 500 m depth (e.g. Badcock
397 and Merrett, 1976; D'Elia *et al.*, 2016).

398 In conclusion the study illustrates the great physical and biological variabilities of the area of eel
399 larvae distribution at STCZ, and points out a range of commonalities and differences between
400 plankton taxa at the mesozooplankton and ichthyoplankton levels. Irrespective of the oligotrophic
401 nature of this oceanic area, the diversity of the plankton community – in terms of taxonomy and
402 distribution patterns - was notably high. Plankton organisms were highly concentrated in specific
403 strata, and several peaks in their vertical distribution could often be seen. These presumably are
404 linked to the variable hydrography around the pycnocline. The anguillid eels concentrate in the
405 lower part of the pycnocline at daytime, and their prevalence in a water layer with enhanced
406 abundances of hydrozoans indicates these organisms as potential prey item for the eel larvae. For
407 further understanding and modelling of the early life characteristics of eel across their extensive
408 area of distribution, it is necessary to incorporate the prominent small-scale variability and diversity
409 of their immediate physical and biological environments.

410

411

412

413 **Acknowledgements**

414 This study was supported by the Carlsberg Foundation, Denmark (2012_01_0272); Danish Centre
415 for Marine Research (2013_02) and the Danish Council for Independent Research/Marie Curie
416 (Mobilex: DFF-1325-00102B to CJ). The authors have no conflicts of interest related to the
417 presented work. We thank colleagues and the crew of the Danish research vessel, DANA, for their
418 helpful assistance during field sampling and sample processing.

419

420 **References**

- 421 Andersen, N. G., Nielsen, T. G., Jakobsen, H. H., Munk, P., & Riemann, L. (2011). Distribution
422 and production of plankton communities in the subtropical convergence zone of the Sargasso Sea.
423 II. Protozooplankton and copepods. *Marine Ecology Progress Series*, 426, 71-86.
- 424 Ayala, D., Riemann, L., & Munk, P. (2016). Species composition and diversity of fish larvae in the
425 Subtropical Convergence Zone of the Sargasso Sea from morphology and DNA barcoding.
426 *Fisheries oceanography*, 25(1), 85-104.
- 427 Ayala, D.J., Munk, P., Lundgreen, R.B.C., Traving, S.J., Jaspers, C., Jørgensen, T.S., Hansen, L.H.
428 & Riemann, L. (in press). Gelatinous plankton is central to the diet of European eel (*Anguilla*
429 *anguilla*) larvae in the Sargasso Sea. *Scientific Reports*
- 430 Badcock, J., & Merrett, N. R. (1976). Midwater fishes in the eastern North Atlantic—I. Vertical
431 distribution and associated biology in 30 N, 23 W, with developmental notes on certain myctophids.
432 *Progress in Oceanography*, 7(1), 3-58.
- 433 Blaxter, J. H. S. (1980). Vision and feeding of fishes. In: *Fish Behaviour and its Use in the Capture*
434 *and Culture of Fishes* (Vol. 5, pp. 32-56). International Center for Living Aquatic Resources
435 Management Manila, Philippines.
- 436 Bouillon, J., Medel, M. D., Pages, F., Gili, J. M., Boero, F. and Gravili, C. (2004) Fauna of the
437 Mediterranean Hydrozoa. *Scientia Marina*, 68, 5-449.
- 438 Castonguay, M., & McCleave, J. D. (1987). Vertical distributions, diel and ontogenetic vertical
439 migrations and net avoidance of leptocephali of *Anguilla* and other common species in the Sargasso
440 Sea. *Journal of Plankton Research*, 9(1), 195-214.
- 441 Cushman-Roisin, B. (1984). On the maintenance of the Subtropical Front and its associated
442 countercurrent. *Journal of physical oceanography*, 14(7), 1179-1190.
- 443 Deevey, G. B., & Brooks, A. L. (1977). Copepods of the Sargasso Sea off Bermuda: species
444 composition, and vertical and seasonal distribution between the surface and 2000 m. *Bulletin of*
445 *Marine Science*, 27(2), 256-291.

446 D'Elia M, Joseph D. Warren, Ivan Rodriguez-Pinto, Tracey T. Sutton, April Cook, Kevin M.
447 Boswell, Diel variation in the vertical distribution of deep-water scattering layers in the Gulf of
448 Mexico, Deep Sea Research Part I: Oceanographic Research Papers, Volume 115, 2016, Pages 91-
449 102, <http://dx.doi.org/10.1016/j.dsr.2016.05.014>.

450 Eriksen, C. C., Weller, R. A., Rudnick, D. L., Pollard, R. T., & Regier, L. A. (1991). Ocean frontal
451 variability in the frontal air-sea interaction experiment. *Journal of Geophysical Research: Oceans*,
452 96(C5), 8569-8591.

453 Gasol JM, del Giorgio PA, Duarte CM (1997) Biomass distribution in marine planktonic
454 communities. *Limnol Oceanogr* 42:1353–1363

455 Halliwell Jr, G. R., Ro, Y. J., & Cornillon, P. (1991). Westward-propagating SST anomalies and
456 baroclinic eddies in the Sargasso Sea. *Journal of physical oceanography*, 21(11), 1664-1680.

457 Jacobsen, M. W., Smedegaard, L., Sørensen, S. R., Pujolar, J. M., Munk, P., Jónsson, B.,
458 Magnussen, E. & Hansen, M. M. (2017). Assessing pre-and post-zygotic barriers between North
459 Atlantic eels (*Anguilla anguilla* and *A. rostrata*). *Heredity*, 118(3), 266.

460 Lawson GL, Peter H. Wiebe, Carin J. Ashjian, Scott M. Gallagher, Cabell S. Davis, Joseph D.
461 Warren, Acoustically-inferred zooplankton distribution in relation to hydrography west of the
462 Antarctic Peninsula, Deep Sea Research Part II: Topical Studies in Oceanography, Volume 51,
463 Issue 17, 2004, Pages 2041-2072,

464 Longhurst, A. R. (1985). The structure and evolution of plankton communities. *Progress in*
465 *Oceanography*, 15(1), 1-35.

466 Miller, M. J. (2015). Nighttime vertical distribution and regional species composition of eel larvae
467 in the western Sargasso Sea. *Regional Studies in Marine Science*, 1, 34-46.

468 Miller, M. J., Bonhommeau, S., Munk, P., Castonguay, M., Hanel, R., & McCleave, J. D. (2014). A
469 century of research on the larval distributions of the Atlantic eels: a re-examination of the data.
470 *Biological Reviews*, 90(4), 1035-1064.

471 Munk, P., Hansen, M. M., Maes, G. E., Nielsen, T. G., Castonguay, M., Riemann, L., ... & Bachler,
472 M. (2010). Oceanic fronts in the Sargasso Sea control the early life and drift of Atlantic eels.
473 *Proceedings of the Royal Society of London B: Biological Sciences*, rspb20100900.

474 Richardson, K., & Bendtsen, J. (2017). Photosynthetic oxygen production in a warmer ocean: the
475 Sargasso Sea as a case study. *Phil. Trans. R. Soc. A*, 375(2102), 20160329.

476 Riemann, L., Nielsen, T. G., Kragh, T., Richardson, K., Parner, H., Jakobsen, H. H., & Munk, P.
477 (2011). Distribution and production of plankton communities in the subtropical convergence zone
478 of the Sargasso Sea. I. Phytoplankton and bacterioplankton. *Marine Ecology Progress Series*, 426,
479 57-70.

480 Rodríguez, J. M., Hernández-León, S., & Barton, E. D. (2006). Vertical distribution of fish larvae in
481 the Canaries-African coastal transition zone in summer. *Marine Biology*, 149(4), 885-897.

482 Sameoto, D. D. (1986). Influence of the biological and physical environment on the vertical
483 distribution of mesozooplankton and micronekton in the eastern tropical Pacific. *Marine Biology*,
484 93(2), 263-279.

485 Schmidt J (1923) The Breeding Places of the Eel. *Philosophical Transactions of the Royal Society*
486 of London. Series B 211: 179-208

487 Schoth, M., & Tesch, F. W. (1982). Spatial distribution of 0-group eel larvae (*Anguilla* sp.) in the
488 Sargasso Sea. *Helgoländer Meeresuntersuchungen*, 35(3), 309.

489 Steinberg, D. K., Carlson, C. A., Bates, N. R., Johnson, R. J., Michaels, A. F., & Knap, A. H.
490 (2001). Overview of the US JGOFS Bermuda Atlantic Time-series Study (BATS): a decade-scale
491 look at ocean biology and biogeochemistry. *Deep Sea Research Part II: Topical Studies in*
492 *Oceanography*, 48(8), 1405-1447.

493 Ullman, D. S., Cornillon, P. C., & Shan, Z. (2007). On the characteristics of subtropical fronts in
494 the North Atlantic. *Journal of Geophysical Research: Oceans*, 112(C1).

495 Williams RG (2001) Ocean subduction. In: Steele JH, Turekian KK, Thorpe SA (eds) *Encyclopedia*
496 *of ocean sciences*. Academic Press, pp 1982–1992

497

498 **Legends to figures**

499

500 **Figure 1**

501 Area of sampling. a) Transect at 62°45'W (line) and sampling position (dot) in the southern
502 Sargasso Sea for this study; contour lines indicate SST from satellite observations. Hydrographical
503 sections along the transect for b) temperature (°C) and c) salinity; vertical lines indicate sampling
504 position for the vertical study

505 **Figure 2**

506 Depth profiles at the vertical study site: a) Temperature, salinity and water density; b) oxygen, light
507 radiance and light attenuation coefficient; c) NO₃+NO₂ and silicate; and d) fluorescence and
508 chlorophyll *a*. Measurements in a) and b) and fluorescence are from CTD cast; measurements in c)
509 and chlorophyll *a* are from water bottle sampling.

510 **Figure 3**

511 Abundances of a) Marine snow (0.05-0.53, 0.53-1.06, 1.06-4.0 mm); b) *Trichodesmium* and
512 Rhizaria; and c) ciliates and heterotrophic dinoflagellates. Measurements in a) and b) are from
513 profiling by video recorder; measurements in c) are from water bottle sampling.

514 **Figure 4**

515 Day (open symbol) and night (closed symbol) vertical distributions of selected plankton taxa and
516 stages. a) to j) Mesozooplankton profiles based on 45 µm vertical Multinet hauls in strata, average
517 abundances in stratum (no. m⁻³). k) and l) Macrozooplankton profiles based on horizontal 550 µm
518 MIK net hauls at depth (no. 1000 m⁻³).

519 **Figure 5**

520 Day-night changes in depth (m) of the abundant copepod taxa. a) Average length (within intervals
521 of 100µm) at depth (m) for all copepods. b) Average depth at day versus night for a number of
522 genera in copepodite stages. c) Average depth at day versus night of adult copepods identified to
523 species.

524 **Figure 6**

525 Vertical distribution and mean sizes of leptocephali species. Day (open symbol) and night (closed
526 symbol) distributions of a) *Anguilla anguilla* and b) *A. rostrata* (no 1000 m⁻³). c) Night distribution
527 of non-anguillid leptocephali larvae (no 1000 m⁻³). d) Mean lengths at depth during day and night
528 for d) *A. anguilla* and f) *A. rostrata* (mm). Based on MIK hauls at nominal depths (symbol ±3m).

529 **Figure 7**

530 Vertical distribution of selected fish larvae species based on MIK hauls at nominal depths (symbol
531 ±3m); values in no. 1000 m⁻³.

532 **Figure 8**

533 Average depth (m) at day versus night for common fish larvae species in the area. The two anguillid
534 species are highlighted by bold text and dashed lines.

535 **Figure 9**

536 Lower graph: Acoustic backscatter by ship-mounted 38KHz echo sounder, in dB, as given by bar to
537 the right. From 01:00 (UTM) on the 31 March to 23:00 on the 1st April. White line off left axis
538 illustrates the salinity profile; lines undulating to depth illustrate calculated depths of given light
539 intensities; white upper line: 1.5 μmol m⁻² s⁻¹, grey lower line: 0.02 μmol m⁻² s⁻¹. Upper graph:
540 surface light intensity during the same period, from ship-mounted PAR sensor.

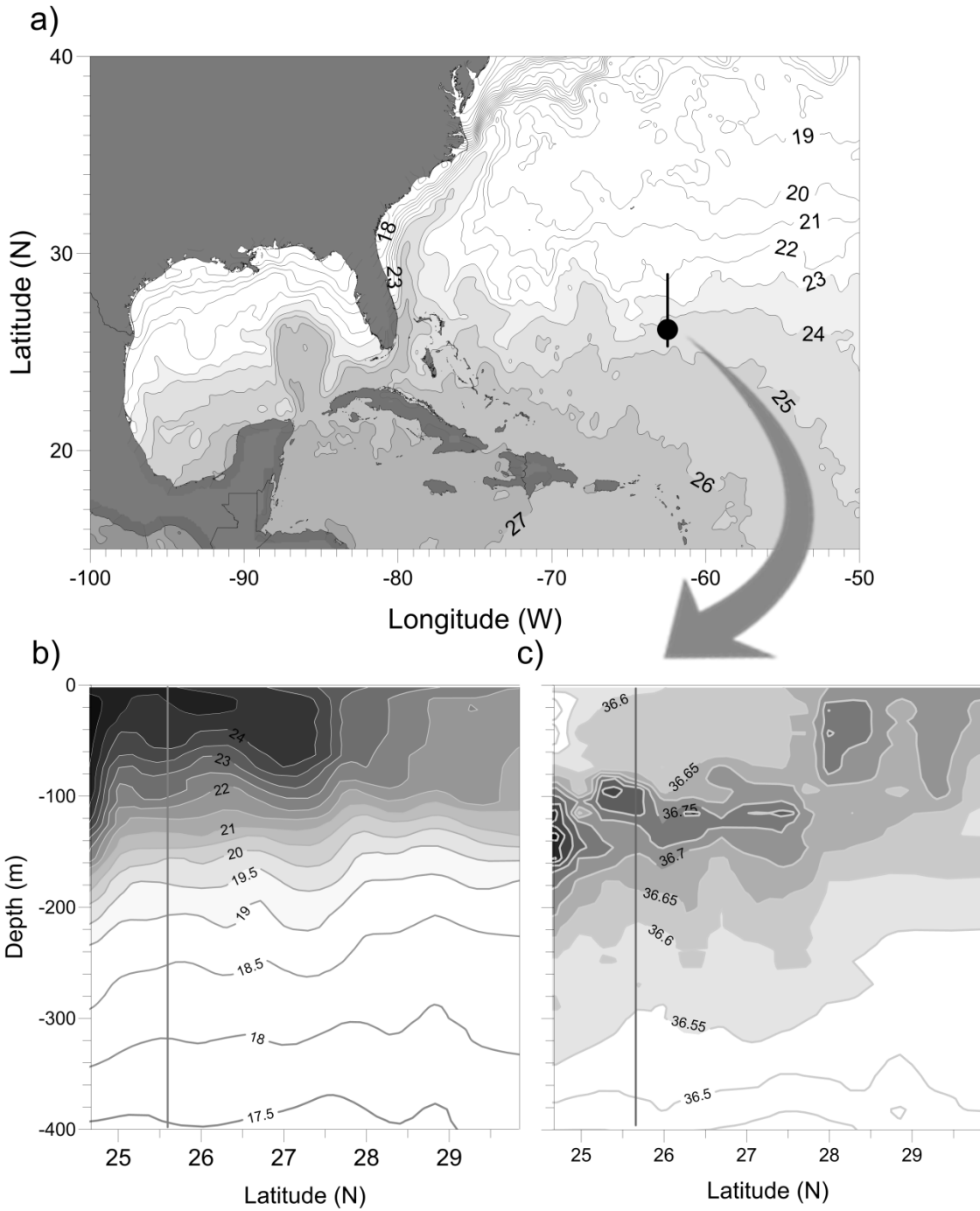
541

542 **Supplementary figure 1.**

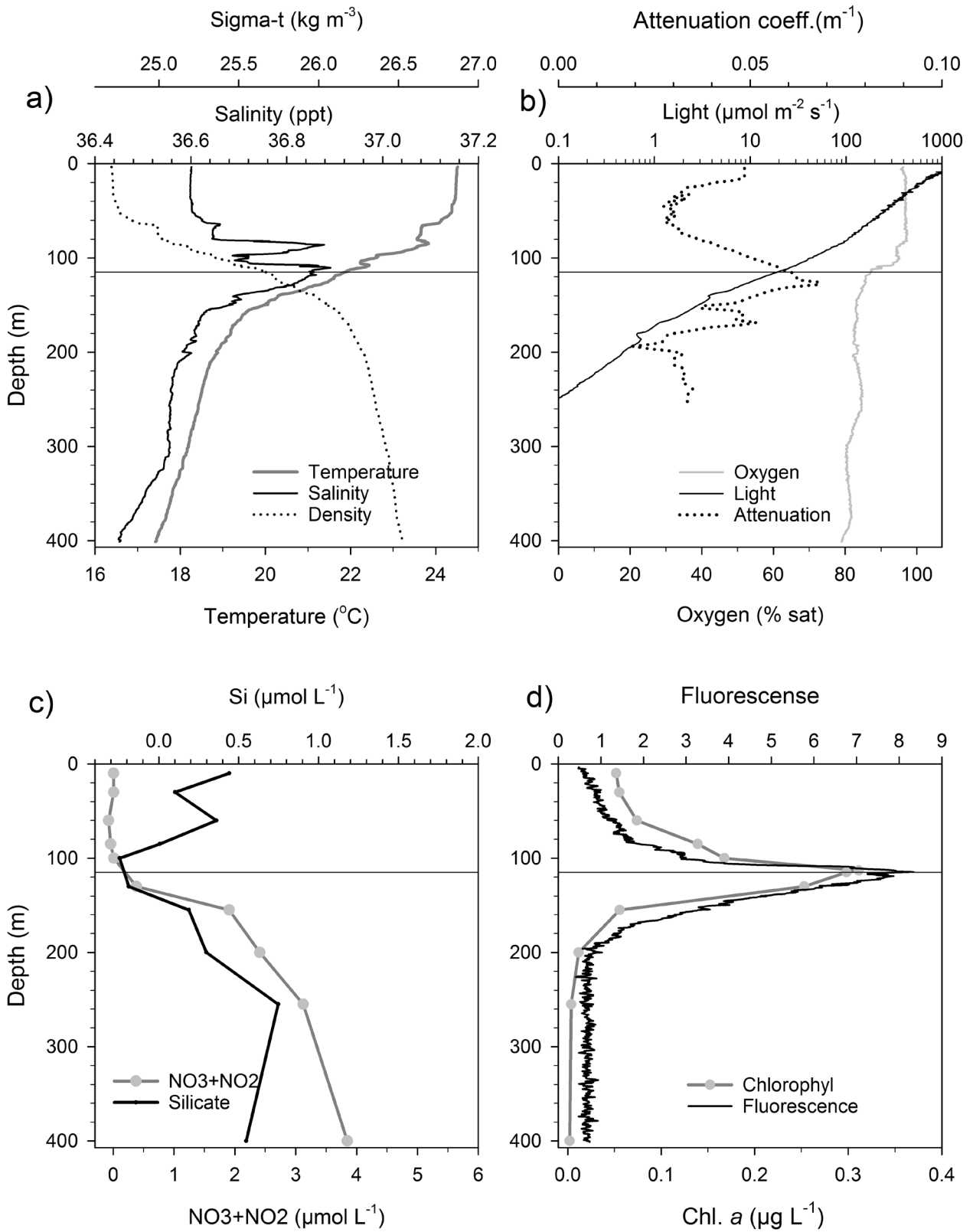
543 Cluster diagrams of relatively abundant plankton taxa (abundance above 10% within three groups:
544 copepods, non-copepod mesozoplankton, and ichthyoplankton). Coloring of presence within the 6
545 strata is represented by a colorbar to the right; presence of each taxon accumulate to 100%. a)
546 Cluster diagram for daytime sampling. Six clusters, separated by >50% level, are marked by red
547 rectangles. Fish larvae taxon is indicated by asterisk. b) Cluster diagram for nighttime sampling.

548 **Supplementary Table 1**

549 Abundances of mesozooplankton (no m^{-3}), macroplankton (no $1000 m^{-3}$) and fish larvae (no 1000
550 m^{-3}) from vertically stratified sampling at average depths 12, 45, 85, 120, 155, 205 and 255 m
551 during day and night periods. The 12 m depth stratum only presented for mesozooplankton.

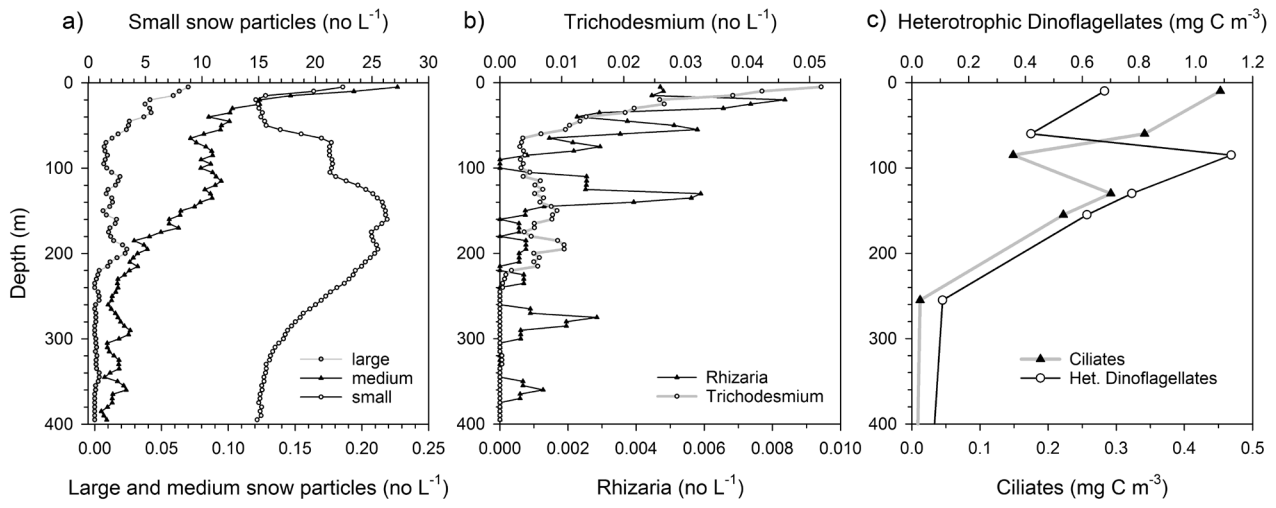


552
553 Figure 1



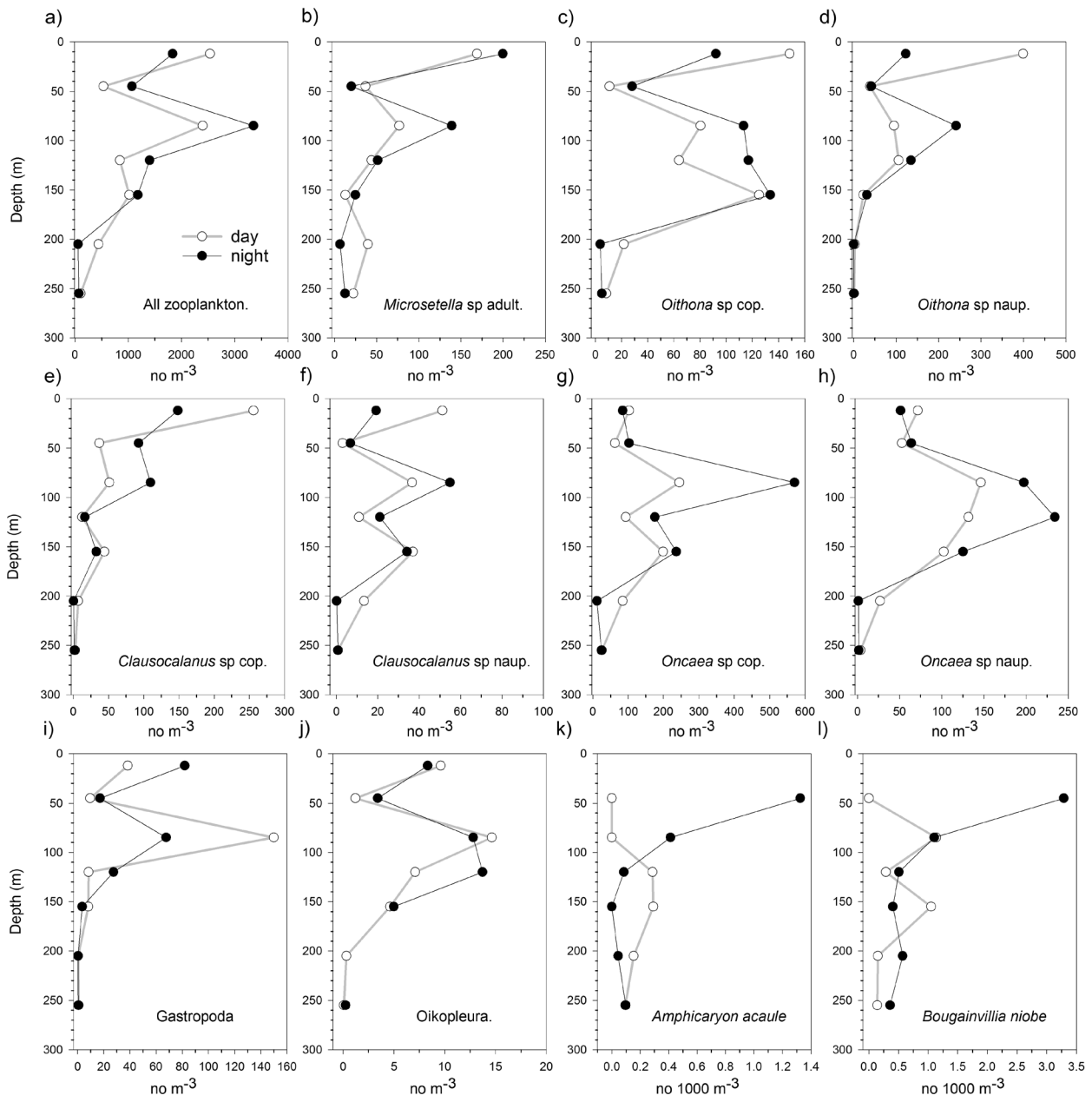
554

555 Figure 2



556

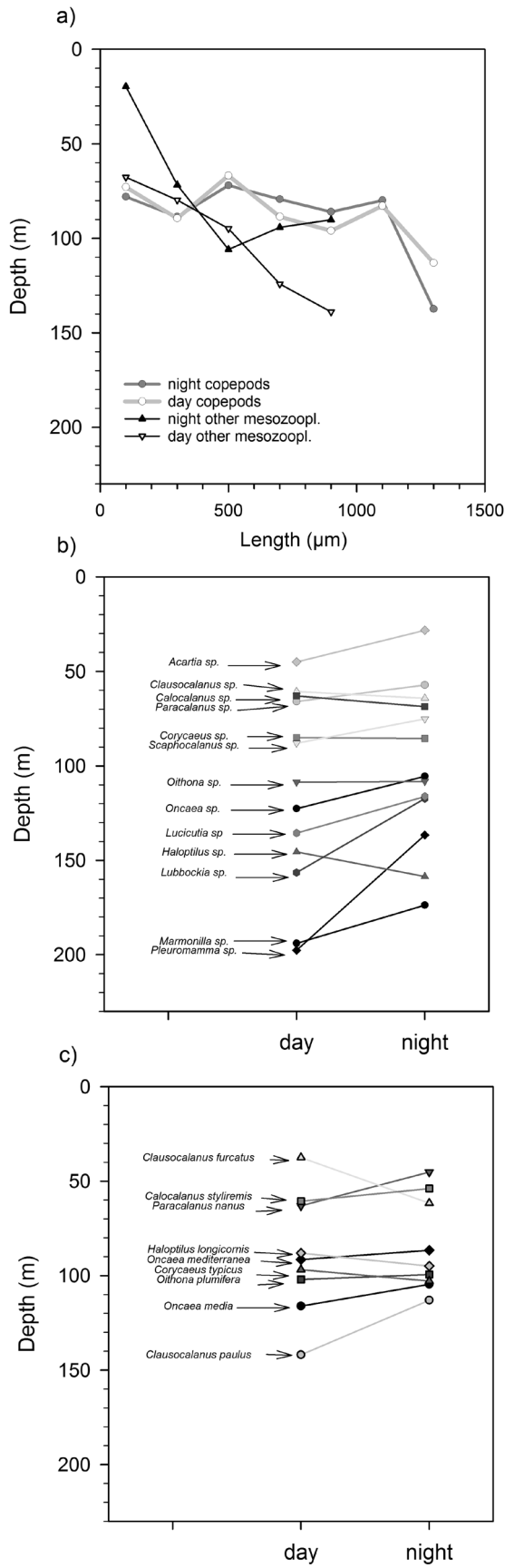
557 Figure 3



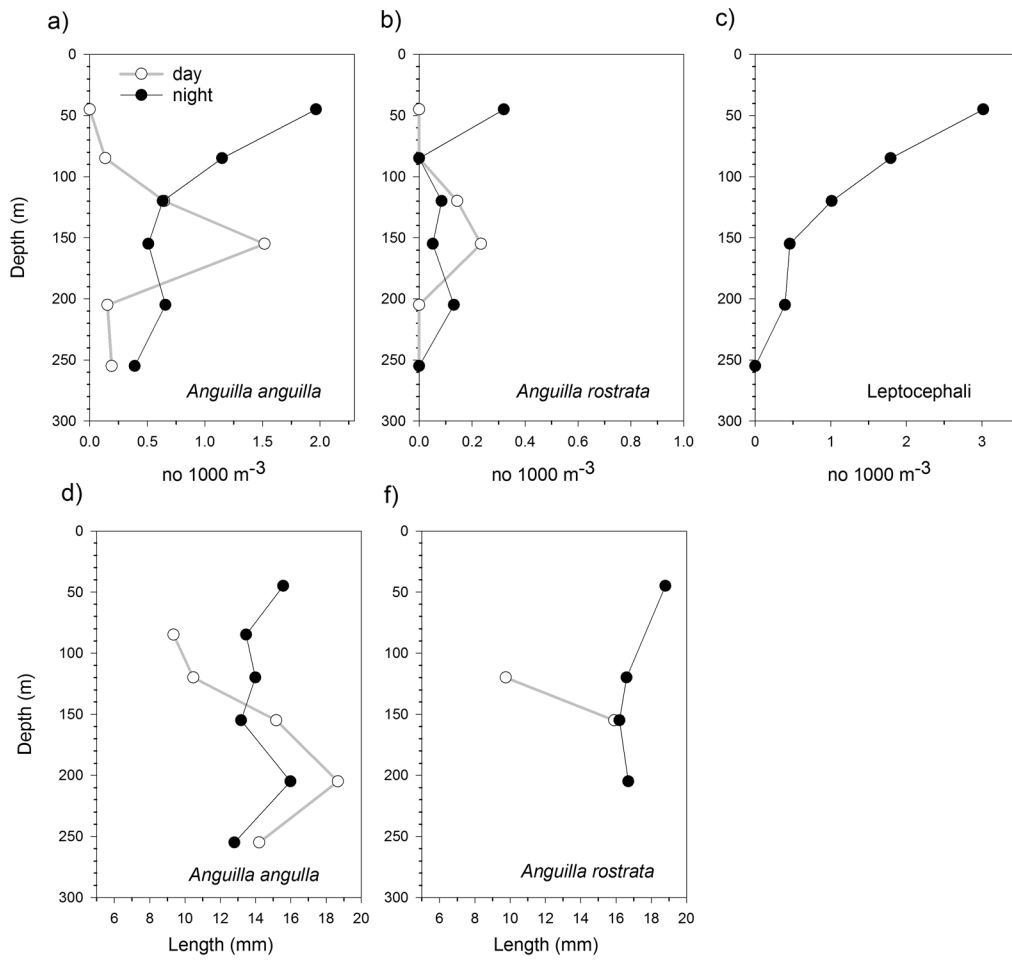
558

559 Figure 4

560

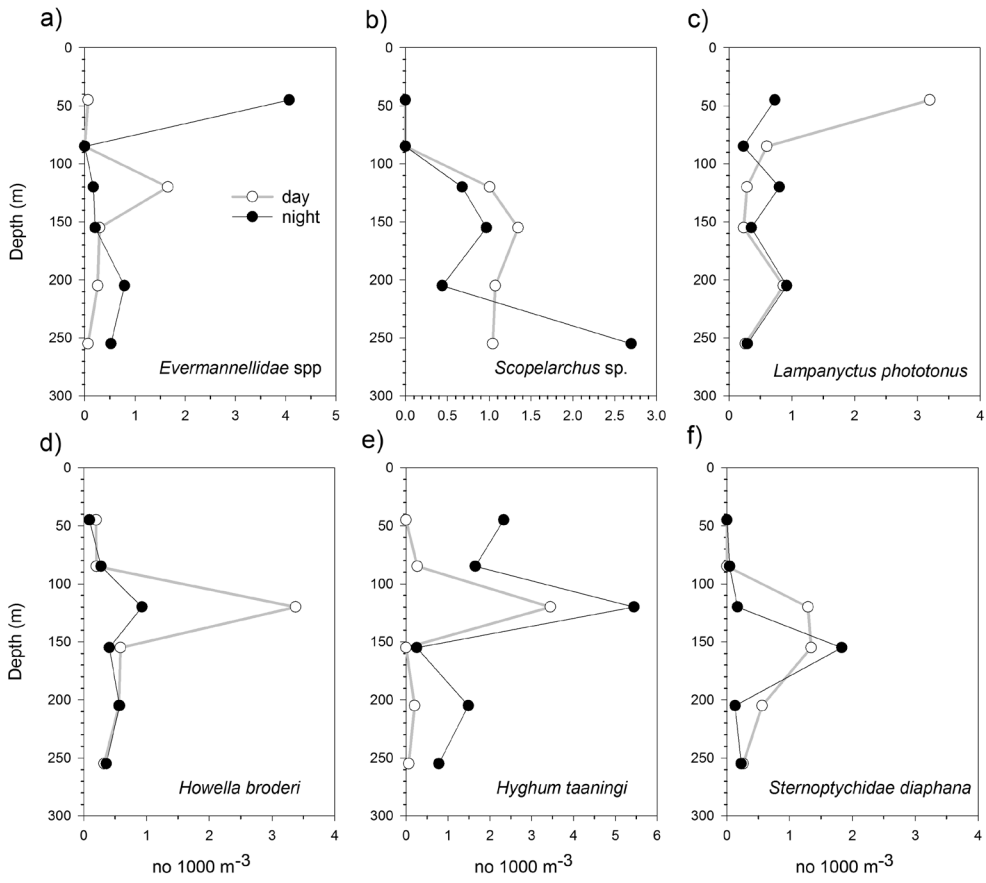


561 Figure 5



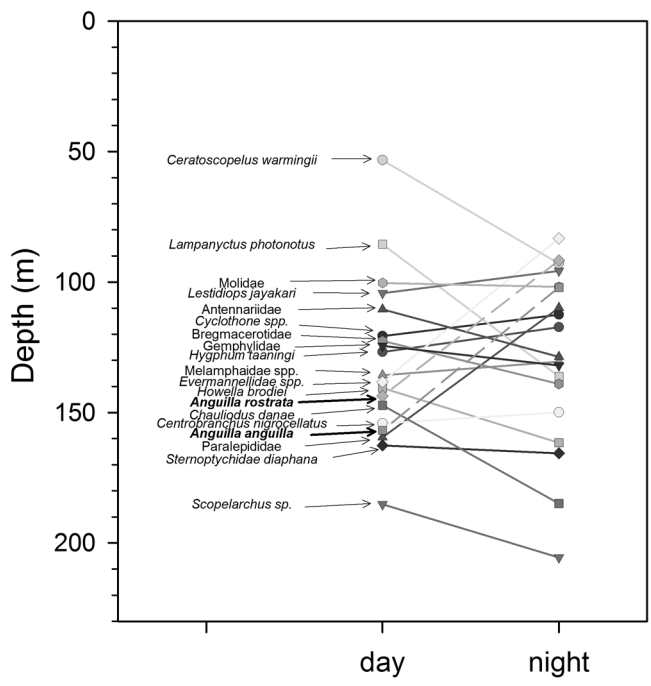
562

563 Figure 6



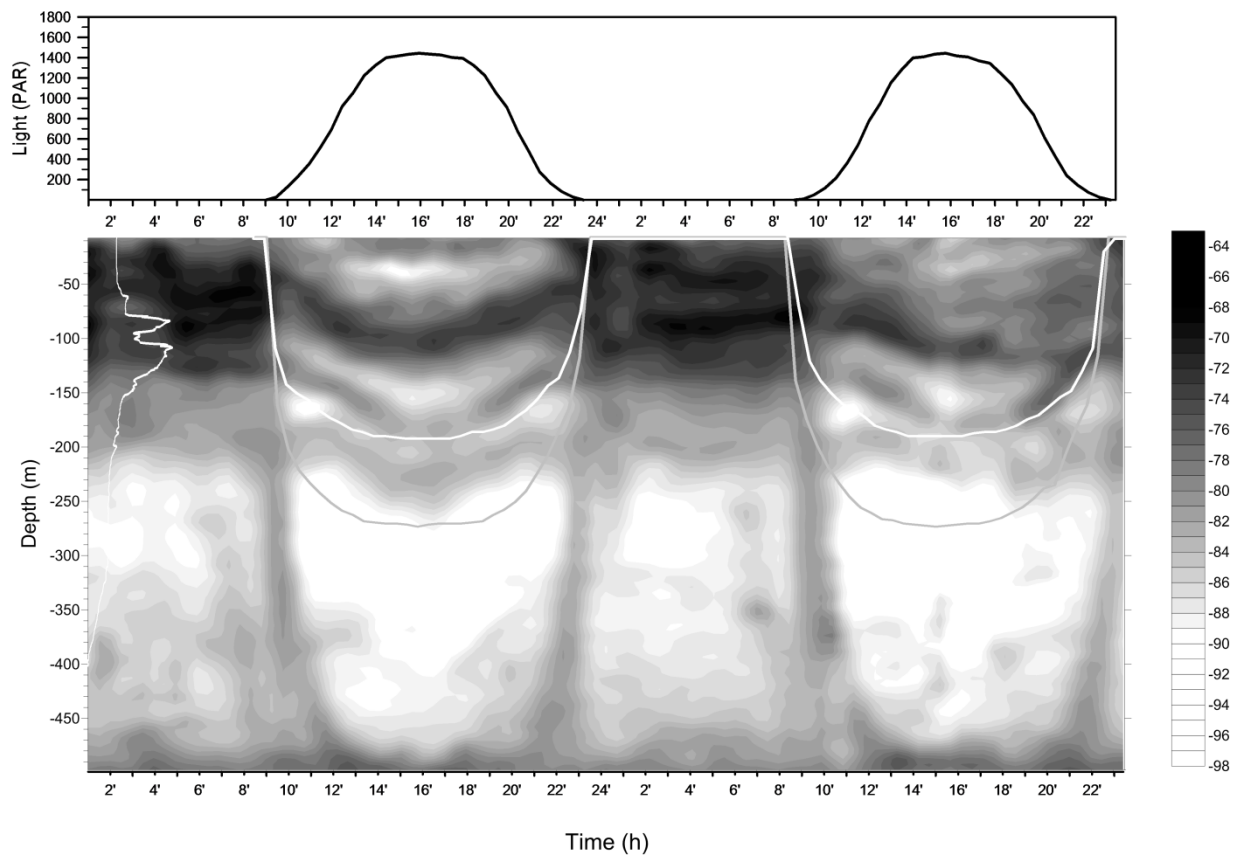
564

565 Figure 7



566

567 Figure 8



568

569 Figure 9

570